Extinction vortices are driven more by a shortage of beneficial mutations than by deleterious mutation accumulation

Walid Mawass[1,2], Joseph Matheson[1,3], Ulises Hernández[1], Jeremy J. Berg[2], Joanna Masel[1]

[1]Department of Ecology and Evolutionary Biology, University of Arizona, Tucson, AZ, 85721, USA
[2]Department of Human Genetics, University of Chicago, Chicago, IL, 60637, USA
[3]Department of Ecology, Behavior, and Evolution, University of California San Diego, San Diego, CA, 92093, USA

Corresponding author: Joanna Masel; masel@arizona.edu

Abstract

Habitat loss contributes to extinction risk in multiple ways. Genetically, small populations can face an "extinction vortex" — a positive feedback loop between declining fitness and declining population size. Two distinct genetic mechanisms can drive a long-term extinction vortex: i) ineffective selection in small populations allows deleterious mutations to fix, driving "mutational meltdown", and ii) smaller populations generate fewer beneficial mutations essential for long-term adaptation, a mechanism we term "mutational drought". To determine their relative importance, we ask whether, for a population near its critical size for persistence, changes in population size have a larger effect on the beneficial vs. deleterious component of fitness flux. In stable environments, we find that mutational drought is nearly as significant as mutational meltdown. Drought is more important than meltdown when populations must also adapt to a changing environment, unless the beneficial mutation rate is extremely high. Linkage disequilibria from background selection under realistically high deleterious mutation rates modestly increase the importance of mutational drought. Long-term conservation efforts should consider adaptive potential, not just deleterious load.

Keywords: population persistence, extinction spiral, population genetics, evolutionary rescue, conservation genetics, background selection

Introduction

To what degree the genetics of a population might contribute to population decline and eventual demise, and how, remains an open question [1–7]. "Extinction vortex" is an umbrella term for a variety of self-reinforcing feedback loops between population size and fitness, including some based on genetics [8]. On short timescales, a population size reduction will increase inbreeding load via deleterious recessive alleles, lowering fitness and potentially reducing population size further [9,10]. On slightly longer timescales, the loss of standing genetic variation can undermine adaptive potential. Here we focus on two even longer-term kinds of extinction vortex, operating over the timescale of fixation events (figure 1). First, ineffective selection in the face of stronger random genetic drift in small populations might allow a series of deleterious mutations to become fixed, in a process of "mutational meltdown". Second, fewer individuals entail fewer opportunities for the appearance of the novel mutations required for long-term adaptation, a process we call "mutational drought".

Mutational meltdown has received the most theoretical attention of the two [11–19]. Mutational meltdown is a positive feedback loop between population size N and mean fitness $\bar{W}$. As a population declines in size, deleterious mutations fix more easily due to random genetic drift (Figure 1, top red blunt arrow ⊥). This decreases mean fitness $\bar{W}$ (Figure 1, bottom red blunt arrow), causing the population size to decline further (Figure 1, upward arrow).

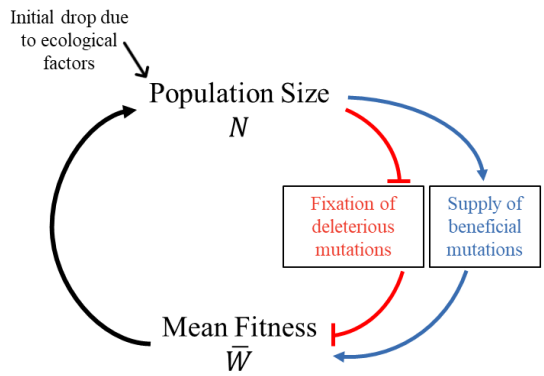

Figure 1. An extinction vortex can be driven by either deleterious (mutational meltdown; red) or beneficial (mutational drought; blue) fixations. When the net effects of deleterious fixations, environmental change, and beneficial fixations cause mean population fitness to decline, the population size N will fall. This fall in N can further exacerbate the tendency for fitness to fall, creating a positive feedback loop (extinction vortex).

Without beneficial mutations, even large populations melt down eventually. This is because some deleterious mutations are too small to be reliably purged by selection, even in large sexual populations; this has been called "Ohta's ratchet" [20]. With a finite number of sites, back mutations could eventually halt this decline, if we ignore essentially irreversible deletions. But for vertebrate parameter values, this comes at the cost of ~100 "lethal equivalents" in the exponent of fitness relative to an individual without deleterious mutations [21]. One proposed solution to this problem [22] unrealistically assumes that unconditionally deleterious mutations do not exist, only mutations to quantitative traits under stabilizing selection.

A more compelling solution is to include larger-effect beneficial mutations, not just reversals [23,24]. This enables compensatory asymmetry, where each larger-effect beneficial fixation offsets the fitness effects of multiple small effect deleterious fixations [24–26]. The effects of deleterious and beneficial fixations on population mean fitness can be captured by their respective "fitness fluxes": $v_d = U_d N \int_{-\infty}^{0} p(s_d) p_{fix}(s_d) s_d \, ds_d$ and $v_b = U_b N \int_{0}^{\infty} p(s_b) p_{fix}(s_b) s_b \, ds_b$, where U_d and U_b give the genome-wide rates of deleterious and beneficial new mutations in each of the N individuals, with selection

coefficients s_d or s_b, respectively, according to probability density function $p(s)$. Mutations fix with probability $p_{fix}(s)$, changing population fitness by s.

Schultz and Lynch [23] emphasized the critical ratio of mutation rates U_b/U_d that is needed to balance deleterious and beneficial fluxes, as a function of population size N and degree of outcrossing. Here we follow Whitlock [24], who studied an essentially identical model, but instead emphasized a critical population size N_{crit} as a function of U_b/U_d. Below N_{crit}, a population with that value of U_b/U_d crosses the threshold into an extinction vortex.

New beneficial mutations create a second, distinct positive feedback loop (Figure 1, blue arrows). Declining N reduces the number of new beneficial mutations, NU_b. (See [27] for empirical support that the beneficial mutation rate can be limiting.) This slows the adaptive increase in $\bar{W}$, which feeds back into lower N (Figure 1, upward arrow). The importance of this second feedback loop was previously briefly noted in the Discussion of [28] as an incidental finding, within a study focused on the effect of fitness function shape on extinction vortices in the context of a rapidly changing environment. We refer to this novel type of extinction vortex as "mutational drought." Adaptive fixations could be in short supply not only to counter environmental change, but also just to offset deleterious fixations under high U_d, even in the absence of environmental change.

Here we ask how important mutational drought is, relative to mutational meltdown. To capture the dynamics of either kind of extinction vortex, fitness must affect population density. In the simplest models of absolute fitness, this leads to unbounded exponential growth for N above a threshold N_{crit}, and so many previous meltdown models study dynamics only once $N < N_{crit}$ [12,13,29]. Here we ignore dynamics and instead take a perturbation approach around the tipping point N_{crit} (which is an unstable equilibrium in phase space), to calculate the derivatives of the two fitness fluxes with respect to population size. A "drought : meltdown ratio" $\left|\frac{dv_b}{dN}/\frac{dv_d}{dN}\right|_{N_{crit}} < 1$ indicates that mutational meltdown is more important in the vicinity of the tipping point, while a ratio > 1 indicates that mutational drought is more important. This perturbation approach allows us to ignore dynamical trajectories. It even allows us to use standard relative fitness models of constant N, under the assumption that first order effects of N on fitness fluxes are larger than second order feedbacks.

Previous models [23,24] of fitness flux $UN\int p(s)p_{fix}(s)s\,ds$ assumed in their calculations of $p_{fix}(s)$ that each mutation evolves independently. However, the independence assumption is violated, even in sexual populations, by background selection caused by deleterious mutations, and by hitchhiking and clonal interference caused by beneficial mutations [30,31]. These phenomena increase the fixation probabilities of deleterious mutations and decrease those of beneficial mutations.

Altered fixation probabilities for both deleterious [32] and beneficial [33] mutations correspond to linkage disequilibrium (LD), i.e. non-independence across sites. Importantly, LD can accelerate mutational meltdown [14]. Empirically, LD has been detected even among unlinked sites [34,35]. Indeed, when $U_d > 1$, more LD is expected from background selection among unlinked sites than from background selection among linked sites in this regime [36].

The evidence for $U_d > 1$ is clearest for humans. A lower bound was derived [37] by assuming that mutations are deleterious only in the 55% of the 6×10^9 base pairs in a diploid genome that are not dominated by dead transposable elements shared with chimpanzees, and that this 55% of the genome evolves 5.7% slower due to this constraint [38], implying that 5.7% of mutations were deleterious enough to be purged by natural selection. A conservative point mutation rate of 1.16×10^{-8} per base pair per replication [39] then yields $U_d > 0.55\times6\times10^9\times0.057\times1.16\times10^{-8} = 2.2$ per replication. This estimate is conservatively low, for five reasons. First, some mutations to transposable element regions are deleterious. Second, 1.16×10^{-8} is the lower bound of a 95% confidence interval on the point mutation rate [39]. Third, non-point mutations and beneficial mutations are neglected. Fourth, the constraint estimate [38] came from reference genomes

that include some derived polymorphisms, which are less constrained than fixed differences. Fifth, under a distribution of fitness effects (DFE), some weakly deleterious mutations fix, and will not be included within the 5.7%. Some therefore argue that the human deleterious mutation rate is as high as $U_d = 10$ [40,41]. Humans have only a modestly higher point mutation rate than most other eukaryotes [39], making it likely that $U_d > 1$ is common.

Capturing unlinked LD arising from $U_d > 1$ requires simulating the entire genome rather than just a genomic region. This is computationally infeasible for most forward-time simulators (e.g., SLiM [42]), because the number of segregating mutations to be tracked scales with $U_d N$, which becomes too large. Here we conduct whole genome simulations using a recently developed approach [26] that assumes that recombination occurs only at hotspots; instead of tracking every segregating mutation, we track only a summary of all mutations to date within each "linkage block" (between hotspots).

Here we ask how important mutational drought is relative to mutational meltdown, as a function of three main factors: 1) U_d/U_b, 2) the rate of environmental change, if any, and 3) the presence or absence of LD. We also confirm that the effect of LD on fitness fluxes and N_{crit} corresponds to that on N_e as assessed the usual way as the expected coalescence time of a neutral allele.

Methods

1. Without linkage disequilibrium (LD)

Fixation probability. Independent evolution of each site (i.e. no LD nor epistasis) enables an analytical, one locus approach. Each copy of a mutation co-dominantly affects fitness by a factor of $(1+s)$, i.e. by $(1+s)^2$ for a homozygous mutant; this convention facilitates comparisons with simulations. The exact probability of fixation $p_{fix}(s)$ of a new mutation under the Moran birth-death process is then $p_{fix}(s) = \frac{1-e^{-s}}{1-e^{-2Ns}}$. We take this from equation 1 of [43], adjusted for a diploid population of size N. It is exact for Malthusian fitness; per-generation fitness yields the same when an approximation is used [44].

Deleterious fitness flux. The best-studied DFE for deleterious mutations was inferred from the human site frequency spectrum of non-synonymous mutations (Table 2, row 9 of [45]). It fits a gamma distribution $p_d(-2N_e s_d) = \frac{e^{\frac{-2N_e s_d}{\beta}} 2N_e s_d{}^{-1+\alpha}\beta^{-\alpha}}{\Gamma(\alpha)}$, where $\Gamma(\alpha)$ is the gamma function, $\alpha = 0.169$ is the shape parameter, and $\beta = 1327.4$ is the scale parameter. We divide by $2N_e$ = 23,646, yielding a DFE for non-synonymous s_d with α = 0.169, β = 0.056.

Many deleterious mutations occur in non-coding regulatory regions such as enhancers and promoters [46], and may have smaller mean deleterious effect size ($\bar{s}_d$) [47]. Structural mutations might have larger $\bar{s}_d$. Departures from co-dominance affect the value of s corresponding to a given value of $p_{fix}(s)$. We therefore explored the sensitivity of our model to the deleterious DFE in two ways: by varying $\bar{s}_d$ (adjusting the scale parameter while keeping the shape parameter fixed), and by varying the coefficient of variation (adjusting both the shape and scale parameters simultaneously to maintain a constant $\bar{s}_d$).

The deleterious fitness flux (v_d) is equal to the per-generation rate of new mutations $U_d N$, times their fixation probability $p_{fix}(s_d)$, times their homozygous impact on fitness $2s_d$ once fixed: $v_d = U_d N \int_{-\infty}^{0} p_d(s_d)\, 2s_d\, p_{fix}(s_d)\, ds_d$. While selective effects $2s_d < -1$ (worse than lethal) form part of the DFE we model, in practice they behave indistinguishably from lethal mutations.

Beneficial fitness flux. We follow others (e.g. [24]) to assume an exponential DFE with mean $\bar{s}_b$, $p_b(s_b) = \frac{1}{\bar{s}_b}\, e^{-s_b/\bar{s}_b}$

to obtain $v_b = U_b N \int_0^{+\infty} p_b(s_b) 2 s_b \, p_{fix}(s_b) \, ds_b$.

Critical population size. We calculated the deleterious and beneficial fitness fluxes numerically in Mathematica 14.2.3 (Supplementary Notebook), using the DFEs $p_d(-2N_e s_d)$ and $p_b(s_b)$, described above. The environmental change rate δ_{env} is either zero or in the range δ_{env}= -10^{-6} to -$10^{-3.5}$. We sometimes express the environmental change rate, for ease in interpretation, as the number of generations over which environmental change reduces fitness by 10%, with -0.1/δ_{env} = 10^5 to $10^{2.5}$ generations. We consider even the fastest of these environmental change rates low because deleterious fixations cause more fitness loss than environmental change does. Coevolution, especially with parasites, likely makes the biggest contribution to δ_{env} [48].

We solve for N_{crit} as the value of N for which $v_{net} = v_b + v_d + \delta_{env} = 0$, and calculate the drought : meltdown ratio as $\left|\frac{dv_b}{dN} \Big/ \frac{dv_d}{dN}\right|_{N_{crit}}$. With linkage equilibrium, $N_e = N$.

The beneficial mutation rate and effect sizes will be larger in worse-adapted populations, but defining a "worse adapted population" is hard within a standard relative fitness formulation of population genetics. Higher U_d and δ_{env} would make populations worse adapted if all else were held equal, but in our modelling framework, these factors are offset by our consideration of perturbation to a higher N_{crit}. Future work on less conventional models of absolute fitness under density-regulation (e.g., [49,50]) would be needed to explore the exact balance between these opposing considerations. Until then, the fact that there is a balance helps justify our use of the same values of U_b and $\bar{s}_b$ as we vary parameters such as U_d and δ_{env}.

2. With LD

Simulation setup. Our forward time simulation method is described in [26]. Briefly, each genome consists of two haplotypes, divided into 23 chromosomes, each further segmented into L = 100 non-recombining 'linkage blocks' (which previous work found to be more than sufficient [26]). To reduce computational load, the fitness impacts of all mutations i within a given allele of linkage block j are not tracked separately, but only via their product $l_j = \prod_i (1 + s_i)$. Recombination occurs only at hotspots between adjacent linkage blocks. We simulated two recombination events per chromosome per meiosis [51].

In each time step of our Moran model, one of the N individuals is chosen uniformly at random to die. To replace it, we select two hermaphroditic parents with probability proportional to their fitness $w = \prod_{j=1}^{L}(l_{j,1}) \prod_{j=1}^{L}(l_{j,2})$, calculated across both haplotypes.

We sampled the numbers of new deleterious and beneficial mutations from Poisson distributions with means U_d and U_b, respectively. We sampled selection coefficients from the same DFEs described in the previous section.

Simulations ran for $100N$ generations. Following [26], we ended a burn-in phase away from a clonal initial population 100 generations after a linear regression of the variance in fitness over the last 200 generations produced a slope less than $0.07/N$. Net fitness flux v_{net} was estimated post burn-in as the slope $\hat{v}_{net}$ of log mean population fitness over time, without decomposition into v_d and v_b.

Critical population size. N_{crit} is defined as the value of N for which $v_{net} = 0$, but $\hat{v}_{net}$ estimation is too noisy to find N_{crit} using purely deterministic root-finding methods, especially for small values of N_{crit}. To account for this stochasticity, we performed 10 independent replicates of the following procedure for each parameter set. We first bracketed N_{crit}, with N = 1500 and 6000 as initial guesses, progressing outward by a factor of two as needed to obtain $\hat{v}_{net}$ values both above and below zero. Then we iterated the secant method until $\hat{v}_{net}$ changed by < 15%. Then we fitted a straight line to all evaluated $\{N, \hat{v}_{net}\}$ data points for which N was within a factor of 3 from the final evaluated value. We estimated N_{crit} for each

replicate as the zero-intercept of this fitted line, and used the mean of these estimates across the 10 replicates for subsequent simulations of matched N.

Drought : meltdown ratio. We estimated v_d and v_b from the set of mutations whose time of final fixation lay between the end of the burn-in phase and the end of the run. Tracking fixations does not exactly track mean population fitness due to fluctuations caused by polymorphisms. For computational efficiency, the linkage block method described so far makes information about individual fixed mutations inaccessible. In simulations intended to estimate the drought : meltdown ratio, we made them accessible via tree sequencing recording [52] tracking all non-neutral mutations, including their time of fixation. We calculated $v_d = \frac{\sum_{i=1}^{n_d} 2s_{d,i}}{G^*}$ and $v_b = \frac{\sum_{i=1}^{n_b} 2s_{b,i}}{G^*}$, where G^* is generations elapsed since burn-in ended, and n_d and n_b are the numbers of deleterious and beneficial mutations that fixed during this time.

We numerically estimated $\frac{dv_b}{dN}$ and $\frac{dv_d}{dN}$ as $\frac{dv}{dN} = \frac{v(N_{crit}+\varepsilon) - v(N_{crit}-\varepsilon)}{2\varepsilon}$, where we chose $\varepsilon = 150$ individuals as a balance between reducing noise and avoiding curvature in v. We did this by running simulations for $N_{crit} + \varepsilon$ and $N_{crit} - \varepsilon$.

Results

Without LD, where $N_e = N$, Whitlock's [24] choice of $U_d/U_b = 1000$, combined with the deleterious DFE from [45], and a conservatively low $\bar{s}_b = 0.001$, with both kinds of mutation co-dominant, yields $N_{crit} \simeq 3666$ (Figure 2A, solid blue and red lines intersecting at dotted red vertical line). An analytical approximation based on an exponential DFE (equation (9) in [24] scaled by 2 to account for the Moran model) underestimates $N_{crit} \cong 2 \times \sqrt[3]{\frac{U_d}{64\,\bar{s}_b{}^2|\bar{s}_d|U_b}} = 2362$. This discrepancy likely arises because our DFE from [45] has a coefficient of variance of 2.4, in contrast to 1 for an exponential distribution. Directly integration of Eq. 3 in [24], which comes prior to the exponential assumption, resolves the discrepancy, to produce $N_{crit} \simeq 3665$. Figure S1 illustrates similar agreement across the range of U_d/U_b values. We note that N_{crit} values in [24] are intended to represent N_e not census N.

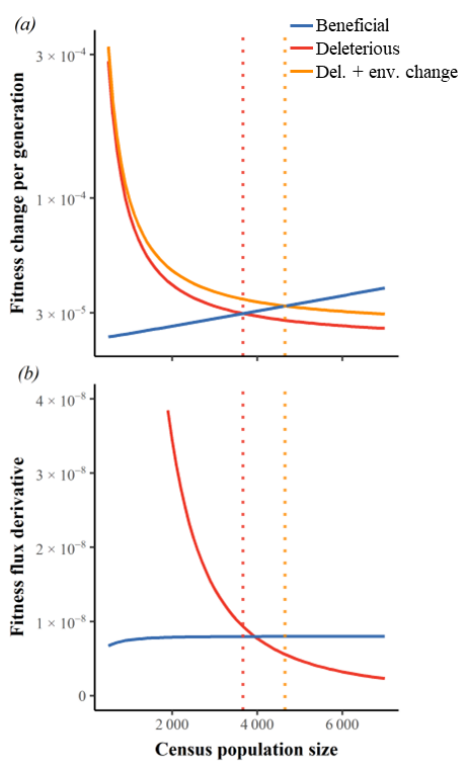

Figure 2. **Extinction vortices are driven more by mutational drought than by mutational meltdown.** Vertical lines indicate N_{crit}, defined by the intersection in (a) of beneficial fitness flux (blue) with either deleterious fitness flux (red), or with deleterious flux plus environmental deterioration (orange). Environmental change adds a constant δ_{env} = -1.5×10^{-5} per generation to deleterious flux in (a) and hence does not change its slope (red line in (b)). The ratio of the y-values in (b) at N_{crit} indicates the relative importance of mutational drought (blue) vs. mutational meltdown (red). U_d = 2, $U_d/U_b = 1000$, $\bar{s}_b$ = 0.001, $\bar{s}_d$ = -0.009 via the DFE from [45], and there is linkage equilibrium.

At N_{crit} in the absence of environmental change (dotted red vertical line in figure 2b), declining N has 85% of the impact on beneficial flux as it has on the deleterious flux that is normally assumed to be the sole cause of an extinction vortex according to mutational meltdown theory. When adaptation must also counter environmental change, larger populations enter the extinction vortex (figure 2a, orange vertical dotted line illustrates $N_{crit} \simeq 4656$ when environmental change reduces fitness by 10% over ~6,000 generations). Even modest environmental change makes the impact of declining N on beneficial flux larger than that on deleterious flux (blue line is above red along dashed orange vertical line in figure 2b). In other words, environmental change makes mutational drought more important than mutational meltdown.

Indeed, the drought : meltdown ratio is > 1 with $U_d/U_b = 1000$ when slow environmental change causes fitness to decline by 10% over as many as ~20,000 generations (figure 3a, right, grey, dot-dashed vertical line). When U_b is 10 times higher, faster but still modest environmental change is needed to drive the drought : meltdown ratio > 1 (figure 3a, left, blue, dot-dashed vertical line, ~4000 generations for fitness to decline by 10%). We interpret both these rates of environmental decline as rather slow because they correspond to only 0.19× and 0.28× the rates of fitness decline due to deleterious fixations for U_d = 2 (figure 3b, colour-matched intersections with vertical lines). Environmental change can drive the drought : meltdown ratio > 1 without excessively elevating N_{crit} (figure 3c steep rise in N_{crit} occurs well to the left of the color-matched vertical line).

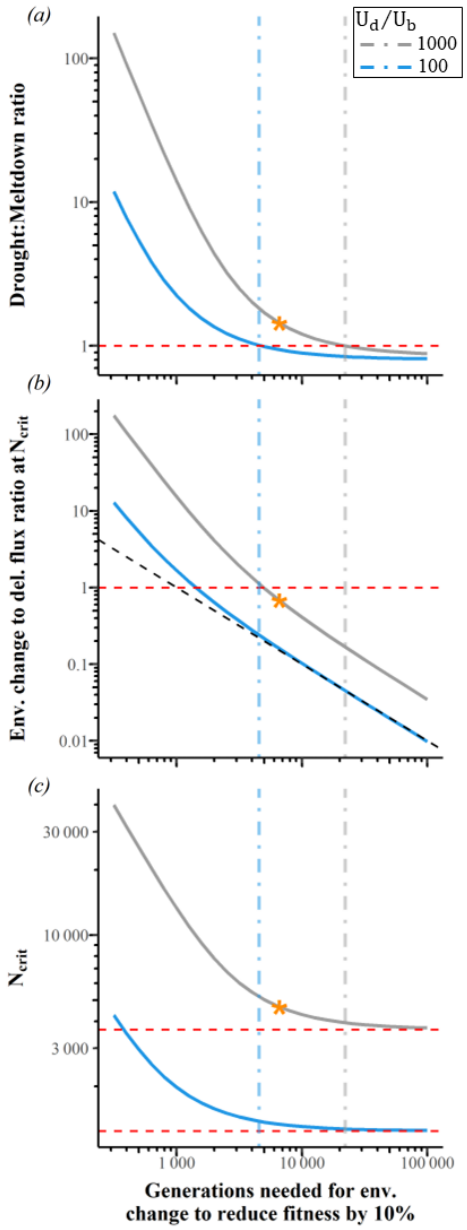

Figure 3. **Slow environmental degradation is sufficient to make mutational drought more important than mutational meltdown.** $\bar{s}_b$ = 0.001, U_d = 2, $\bar{s}_d$ = -0.009 via the DFE from [45]. Linkage equilibrium is assumed. The orange star indicates the example shown in figure 2. Vertical lines represent where the drought : meltdown ratio = 1. (b) We consider environmental change to be relatively slow below the red dashed horizontal line, where mutational degradation makes a bigger contribution to fitness decline. Diagonal black dashed line in (b) represents proportionate change in the x-axis and y-axis; departure from this indicates increased deleterious flux in the face of rapid adaptation. Red dashed lines in (c) indicate asymptotes, i.e. no environmental change.

When beneficial mutations are scarce (higher U_d/U_b), mutational drought is relatively more important, with the drought : meltdown ratio saturated by the U_d/U_b~1000 value (figure 4a) used in figure 2. Lowering U_b has two opposing effects. First, it proportionately lowers the beneficial fitness flux v_b and its derivative $\frac{dv_b}{dN}$ (i.e. it reduces the slope of the blue line in figures 2A and consequently reduces the height of the blue line in figure 2B). Second, lower v_b moves the intersection N_{crit} to the right, i.e. towards larger values of N, which lowers $\left.\frac{dv_d}{dN}\right|_{N_{crit}}$ without substantially changing $\left.\frac{dv_b}{dN}\right|_{N_{crit}}$ (figure 2B, red and blue lines,

respectively). The flat drought : meltdown ratio to the right of figure 4a shows that when beneficial mutations are scarce at high $U_d/U_b \geq 1000$, these two effects cancel each other out.

Weaker beneficial effects (figure 4b), and stronger deleterious effects (figure 4c) make mutational drought only slightly less important. These effects are only slightly larger when beneficial mutations are more common (figures 4b and 4c dashed curves). This makes our results insensitive to the difficulties of empirically inferring selective effect sizes and their dominance coefficients, and to the fact that global epistasis might cause selective effect sizes to vary across scenarios. Mutational drought is relatively more important when the deleterious DFE has a higher coefficient of variation, while holding $\bar{s}_d$ constant (Figure S3). The non-synonymous DFE we use from [45] is overdispersed, and mixing this with DFEs of different $\bar{s}_d$ is likely to further increase the overdispersion.

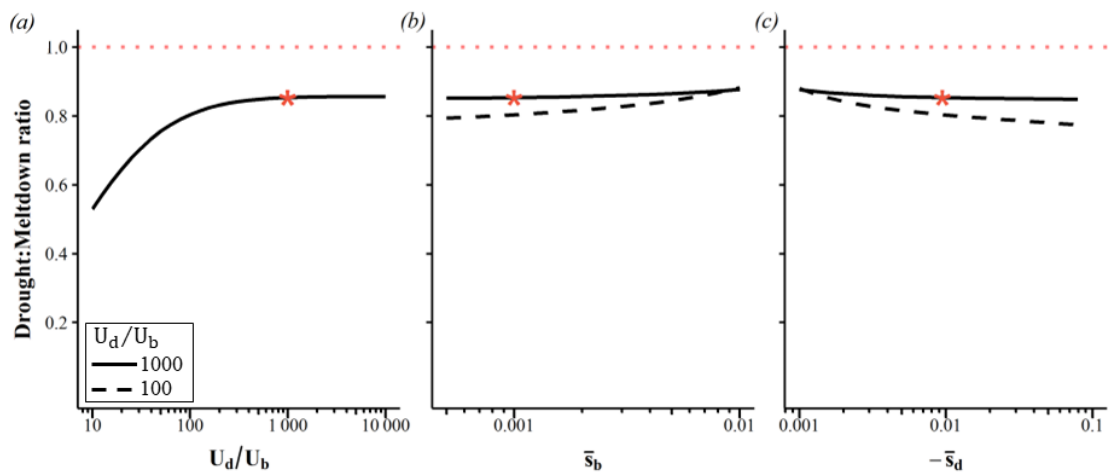

Figure 4. **The drought : meltdown ratio is fairly insensitive to parameter value choices.** Linkage equilibrium is assumed, with no environmental change. (a) Mutational drought becomes somewhat less important when (a) beneficial mutations are abundant, (b) beneficial effects are weak, and (c) deleterious effects are strong. Where not otherwise specified, $\bar{s}_d$ = 0.009 via the DFE from [45], $\bar{s}_b$ = 0.001. U_d = 2 throughout, but results for different U_d are superimposable. The red star indicates the example shown in figure 2 with no environmental change. See figure S2 for corresponding changes in N_{crit}.

With environmental change, dependence on U_d and U_b does not simplify to dependence on their ratio, as in figure 4a. When faster environmental change and more scarce beneficial mutations push the drought : meltdown ratio above 1 (figures 5a and 5b), lower U_d makes mutational drought more rather than less important (figure 5a). The drought : meltdown ratio only falls substantially below 1 under the slower environmental change scenario, and only when U_d/U_b is small (figure 5a, left portion of dashed blue). This scenario entails exceptionally small N_{crit} (figure 5e). Under realistically high U_d, high drought : meltdown ratios are found when beneficial mutations are scarce (figure 5b, solid lines to right), making N_{crit} high (figure 5f), and thus environmental change at N_{crit} is relatively fast compared to a slower rate of deleterious fixations (figure 5d). The drought : meltdown ratio is mostly insensitive to selection coefficients, although it rises for very small $\bar{s}_b$ (figure S4).

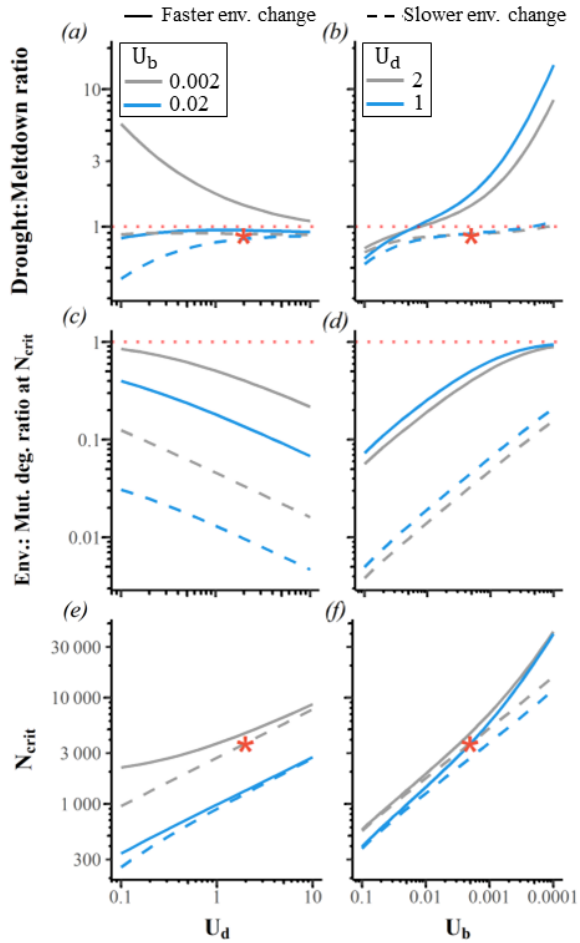

Figure 5. The drought : meltdown ratio only falls substantially below 1 for slower environmental change, and only when U_d/U_b is small. (a) Faster environmental degradation, combined with low U_b, can make mutational drought more rather than less important for lower U_d. (a) and (d) can be compared to the constant environment in figure 4a, where only the ratio U_d/U_b matters. Reverse scaling of the U_b x-axis of (d-f) is used to facilitate comparison of (d) with (a) and with figure 4a. In our "fast" environmental change scenario (solid lines; δ_{env}= -1.5×10^{-5} per generation, matching the example in figure 2), fitness loss from environmental degradation is comparable to, though still slower than, fitness loss from deleterious fixations (y-axis values modestly <1 in (c-d)). In our "slow" scenario (dashed lines; δ_{env} = -10^{-6}), environmental degradation is much slower than mutational degradation (c-d), making results comparable to the constant environment example from figure 2 (red star). Independent sites model with $\bar{s}_b$ = 0.001 and $\bar{s}_d$ = -0.009 via the DFE from [45].

The presence of LD, which we capture in simulations with U_d = 2 and no environmental change, produces a modest 8% increase in the drought : meltdown ratio, from 0.85 to 0.92, as beneficial flux becomes slightly more sensitive to N (figure 6d, blue points are above blue line). This goes away when we quantitatively reduce LD by increasing the number of chromosomes from 23 to 50 (figure S4a).

LD increases N_{crit} from 3666 to 4613 (figure 6a, solid dots), in a way that is qualitatively robust to adding more chromosomes (figure S4b). The $N = 4613$ population with LD can thus been seen to have $N_e = 3666$, such that $\frac{N_e}{N} = \frac{3666}{4613}$. Beyond N_{crit}, rescaling describes v_d and v_b well, as seen by the close match between analytical lines and simulated points when the x-axes of figures 6a and 6c are rescaled according to $N_e = N\frac{\text{analytical } N_{crit}}{\text{simulated } N_{crit}}$ to produce figures 6b and 6d. LD slightly increases the magnitude of fitness fluxes at their $v_d = v_b$ intersection (figure 6b).

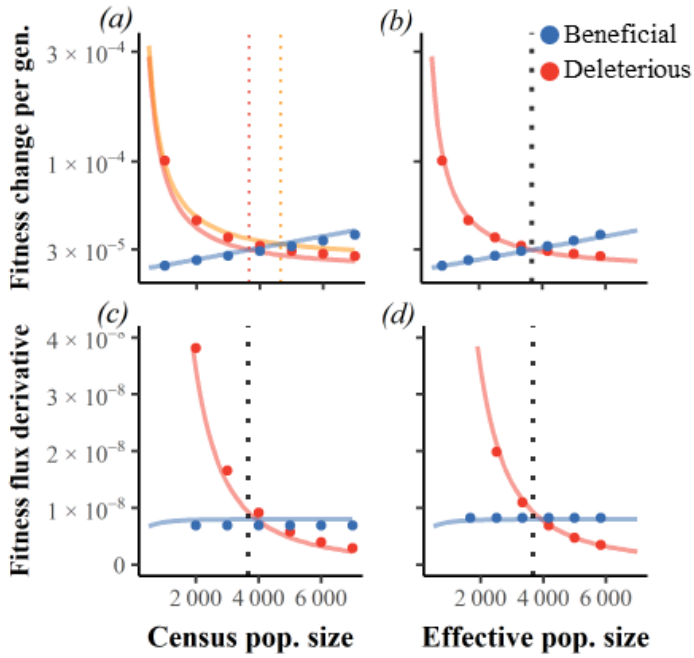

Figure 6. Fitness fluxes scale with effective population size under linkage disequilibrium. Continuous red and blue lines are analytical results given linkage equilibrium, while dots are simulation results with LD. (a) and (b) add simulation results to the static environment example of figure 2. In (c) and (d), the x-axis for simulation results is scaled such that intersection occurs at the same "effective" N_{crit} as found without LD. Linkage disequilibrium makes mutational drought slightly more important. U_d = 2, $U_d/U_b = 1000$, $\bar{s}_b$ = 0.001, $\bar{s}_d$ = -0.009 via the DFE from [45].

The reduction in N_e could be due to beneficial mutations interfering with each other (clonal interference decreasing beneficial flux), and/or hitchhiking (beneficial mutations increasing deleterious flux), and/or background selection (deleterious mutations both decreasing beneficial flux and increasing deleterious flux). We assessed N_e in control simulations with $U_b = 0$, while using matching values of $N = N_{crit}$ in the corresponding scenario with $U_b > 0$. Equal values of coalescent N_e/N in these controls (figure S6, red vs blue) points to background selection as the cause. Assessing N_e via the reduction in fitness fluxes (figure S6, black circles) yields similar values of N_e/N.

Discussion

Mutational meltdown describes an extinction vortex in which small populations cannot purge slightly deleterious mutations, whose fixations handicap the population, making it still smaller. Here, we find that a shortage of beneficial mutations appearing in smaller populations creates mutational drought, a distinct kind of extinction vortex. Mutational drought is only slightly less significant than mutational meltdown in the absence of environmental change, and becomes more important in the more realistic scenario of even a slowly changing environment. Mutational drought is modestly more significant with LD, and more significant when beneficial mutations are rare. Beneficial mutations are thus either common, or else their population-size-dependent scarcity is critical – in neither case can population genetic models ignore beneficial mutations. The relative roles of drought and meltdown are remarkably insensitive to selection coefficients, and only modestly dependent on the relatively frequencies of beneficial vs. deleterious mutations. The greatest parameter value sensitivity is to the rate of environmental change, which if fast, can drive a huge excess of drought over meltdown.

We have ignored population structure. In structured populations, the synergistic interaction between mutation accumulation and demography makes fragmented metapopulations more vulnerable to extinction

than panmictic populations of equivalent size [53]. However, fragmentation might not affect mutational drought the same way. Indeed, in asexual populations, fragmentation has been empirically found to improve adaptation given ruggedness of the fitness landscape [54]. When environments vary among demes, high dispersal can trigger a 'migrational meltdown' by swamping local adaptation [55]. On the other hand, under hard selection, high migration rates are required to buffer demes against local mutational meltdown [56]. It is not yet known what migration rates are needed to similarly buffer demes against local mutational drought.

The role of beneficial mutations in population persistence studied here plays out over much longer timescales than processes of "evolutionary rescue" in previous population genetic (discrete) models, although in line with the broader use of the same term in the context of quantitative genetics models (see [28]). In the broad sense, evolutionary rescue refers to scenarios where genetic adaptation struggles to keep up with ongoing environmental change, over an indefinitely long period of time [57–61]. Within the narrow sense, population genetic models of evolutionary rescue consider a population whose birth rate is initially less than its death rate, e.g. following a single abrupt environmental change that can be remedied by one or several beneficial mutation(s) [62–67]. Here we used a population genetic model to consider evolutionary rescue in the broad sense more commonly treated by quantitative genetic models, across an indefinitely long series of beneficial and deleterious fixations.

Conservation management and species recovery programs assess the 'minimum viable population' and the factors influencing it [68–71]. We follow [72] in defining N_{crit} as the lowest population size that avoids an extinction vortex. This is a different kind of minimum viable population to the usually considered empirical predictor of probability of persistence after a specified period of time, e.g. 1000 years [71,73]. Our N_{crit} concerns the ability to resupply the population with new beneficial mutations to balance both the accumulation of deleterious mutations, and ongoing environmental change, to achieve long-term viability. N_{crit} is the gateway to the extinction vortex below which some combination of mutational meltdown and mutational drought contribute. Our N_{crit} is relevant over the long timescales of multiple sweeps, making our results applicable more clearly to species than to populations, reliant on mutation rather than migration as the source of new variants.

The assessed extinction risk of vertebrate species in the Anthropocene [74] includes assessed long-term risks to environmental conditions [75]. Current conservation efforts often focus on emergency revitalization programs with tools that might only achieve short-term persistence (e.g., [76]), potentially creating trade-offs between long-term and short-term objectives [77]. Short-term goals may be problematically prioritized under triage from restricted budgets [78,79] over achieving long-term sustainable populations [80,81].

Some conservation geneticists advocate genetic rescue, whereby gene flow from a few introduced individuals helps small fragmented populations [82–84]. The genetic rescue paradigm aims to maximize genetic diversity to reduce the risk of extinction [82,85,86]. However, gene flow from large, outbred populations may introduce too many recessive deleterious alleles to be easily purged, with deleterious effects that might quickly have devastating consequences within a small inbred population [6,87,88]. Abandoning the genetic rescue paradigm might limit the risk of deleterious accumulation in the short term. Our results on mutational drought help emphasize that this might still be a mistake over longer timescales if a shortage of adaptive mutations later poses an extinction risk. Fortunately, according to simulations, the benefits of genetic rescue can be obtained while minimizing harm by steadily introducing migrants from other small inbred populations from which recessive deleterious mutations are already purged [6,88], as has occurred naturally in Florida scrub-jays [89].

Acknowledgements

We thank Daniel Smith, Ryan Gutenkunst, Elise Lauterbur, and David Enard for their thoughtful comments on parts of this study, and Naman Panday for sharing his git expertise. We also thank Jerome Kelleher,

Peter Ralph, and Yan Wong for helpful discussions about tree sequence recording. Finally, we extend our thanks to the anonymous reviewers, whose comments which have greatly improved this work.

Funding

This study was funded by the John Templeton Foundation (62028) and by NIH R35 grant (GM151257). The funders had no role in study design, data collection and analysis, decision to publish, or preparation of the manuscript.

Data Availability

Analytical results conducted in Wolfram Mathematica. Simulation code was written in C, and graphs produced with R. Simulation code and scripts have been archived at [90].

Conflict of interest

All authors declare no conflicts of interest.

References

1. Keller LF, Waller DM. 2002 Inbreeding effects in wild populations. *Trends Ecol. Evol.* **17**, 230–241. (doi:10.1016/S0169-5347(02)02489-8)

2. Spielman D, Brook BW, Frankham R. 2004 Most species are not driven to extinction before genetic factors impact them. *Proc. Natl. Acad. Sci.* **101**, 15261–15264. (doi:10.1073/pnas.0403809101)

3. Frankham R. 2005 Genetics and extinction. *Biol. Conserv.* **126**, 131–140. (doi:10.1016/j.biocon.2005.05.002)

4. Fox CW, Reed DH. 2011 Inbreeding Depression Increases with Environmental Stress: An Experimental Study and Meta-analysis. *Evolution* **65**, 246–258. (doi:10.1111/j.1558-5646.2010.01108.x)

5. Kardos M, Armstrong EE, Fitzpatrick SW, Hauser S, Hedrick PW, Miller JM, Tallmon DA, Funk WC. 2021 The crucial role of genome-wide genetic variation in conservation. *Proc. Natl. Acad. Sci.* **118**, e2104642118. (doi:10.1073/pnas.2104642118)

6. Kyriazis CC, Wayne RK, Lohmueller KE. 2021 Strongly deleterious mutations are a primary determinant of extinction risk due to inbreeding depression. *Evol. Lett.* **5**, 33–47. (doi:10.1002/evl3.209)

7. Dussex N, Morales HE, Grossen C, Dalén L, Oosterhout C van. 2023 Purging and accumulation of genetic load in conservation. *Trends Ecol. Evol.* **38**, 961–969. (doi:10.1016/j.tree.2023.05.008)

8. Giplin ME, Soulé ME. 1986 Minimum viable populations : Processes of species extinction. *Conserv. Biol. Sci. Scarcity Divers.* , 19–34.

9. Tanaka Y. 2000 Extinction of populations by inbreeding depression under stochastic environments. *Popul. Ecol.* **42**, 55–62. (doi:10.1007/s101440050009)

10. Fagan WF, Holmes EE. 2006 Quantifying the extinction vortex. *Ecol. Lett.* **9**, 51–60. (doi:10.1111/j.1461-0248.2005.00845.x)

11. Lynch M, Gabriel W. 1990 Mutation Load and the Survival of Small Populations. *Evolution* **44**, 1725–1737. (doi:10.1111/j.1558-5646.1990.tb05244.x)

12. Gabriel W, Lynch M, Bürger R. 1993 Muller's Ratchet and Mutational Meltdowns. *Evolution* **47**, 1744–1757. (doi:10.1111/J.1558-5646.1993.TB01266.X)

13. Lynch M, Conery J, Bürger R. 1995 Mutational Meltdowns in Sexual Populations. *Evolution* **49**, 1067–1080. (doi:10.1111/j.1558-5646.1995.tb04434.x)

14. Lynch M, Conery J, Bürger R. 1995 Mutation Accumulation and the Extinction of Small Populations. *Am. Nat.* **146**, 489–518.

15. Zeyl C, Mizesko M, De Visser JAGM. 2001 Mutational Meltdown in Laboratory Yeast Populations. *Evolution* **55**, 909–917. (doi:10.1111/j.0014-3820.2001.tb00608.x)

16. Shaw FH, Baer CF. 2011 Fitness-dependent mutation rates in finite populations. *J. Evol. Biol.* **24**, 1677–1684. (doi:10.1111/j.1420-9101.2011.02320.x)

17. Coron C, Méléard S, Porcher E, Robert A. 2013 Quantifying the Mutational Meltdown in Diploid Populations. *Am. Nat.* **181**, 623–636. (doi:10.1086/670022)

18. Lansch-Justen L, Cusseddu D, Schmitz MA, Bank C. 2022 The extinction time under mutational meltdown driven by high mutation rates. *Ecol. Evol.* **12**, e9046. (doi:10.1002/ece3.9046)

19. Olofsson P, Chipkin L, Daileda RC, Azevedo RBR. 2023 Mutational meltdown in asexual populations doomed to extinction. *J. Math. Biol.* **87**, 88. (doi:10.1007/s00285-023-02019-y)

20. Ruan Y, Wang H, Zhang L, Wen H, Wu C-I. 2020 Sex, fitness decline and recombination – Muller's ratchet vs. Ohta's ratchet. , 2020.08.06.240713. (doi:10.1101/2020.08.06.240713)

21. Kondrashov AS. 1995 Contamination of the genome by very slightly deleterious mutations: why have we not died 100 times over? *J. Theor. Biol.* **175**, 583–594. (doi:10.1006/jtbi.1995.0167)

22. Charlesworth B. 2013 Why We Are Not Dead One Hundred Times Over. *Evolution* **67**, 3354–3361. (doi:10.1111/evo.12195)

23. Schultz ST, Lynch M. 1997 Mutation and Extinction: The Role of Variable Mutational Effects, Synergistic Epistasis, Beneficial Mutations, and Degree of Outcrossing. *Evolution* **51**, 1363–1371. (doi:10.1111/j.1558-5646.1997.tb01459.x)

24. Whitlock MC. 2000 Fixation of New Alleles and the Extinction of Small Populations: Drift Load, Beneficial Alleles, and Sexual Selection. *Evolution* **54**, 1855–1861.

25. Poon A, Otto SP. 2000 Compensating for Our Load of Mutations: Freezing the Meltdown of Small Populations. *Evolution* **54**, 1467–1479. (doi:10.1111/j.0014-3820.2000.tb00693.x)

26. Matheson J, Hernández U, Bertram J, Masel J. 2025 Human deleterious mutation rate slows adaptation and implies high fitness variance. *bioRxiv* , 2023.09.01.555871. (doi:10.1101/2023.09.01.555871)

27. Rousselle M, Simion P, Tilak M-K, Figuet E, Nabholz B, Galtier N. 2020 Is adaptation limited by mutation? A timescale-dependent effect of genetic diversity on the adaptive substitution rate in animals. *PLOS Genet.* **16**, e1008668. (doi:10.1371/journal.pgen.1008668)

28. Osmond MM, Klausmeier CA. 2017 An evolutionary tipping point in a changing environment. *Evolution* **71**, 2930–2941. (doi:10.1111/evo.13374)

29. Lande R. 1994 Risk of population extinction from fixation of new deleterious mutations. *Evolution* **48**, 1460–1469. (doi:10.1111/J.1558-5646.1994.TB02188.X)

30. Park S-C, Krug J. 2007 Clonal interference in large populations. *Proc. Natl. Acad. Sci.* **104**, 18135–18140. (doi:10.1073/pnas.0705778104)

31. Charlesworth B, Jensen JD. 2021 Effects of Selection at Linked Sites on Patterns of Genetic Variability. *Annu. Rev. Ecol. Evol. Syst.* **52**, 177–197. (doi:10.1146/annurev-ecolsys-010621-044528)

32. Keightley PD, Otto SP. 2006 Interference among deleterious mutations favours sex and recombination in finite populations. *Nature* **443**, 89–92. (doi:10.1038/nature05049)

33. Barton NH, Otto SP. 2005 Evolution of Recombination Due to Random Drift. *Genetics* **169**, 2353–2370. (doi:10.1534/genetics.104.032821)

34. Sohail M *et al.* 2017 Negative selection in humans and fruit flies involves synergistic epistasis. *Science* **356**, 539–542. (doi:10.1126/science.aah5238)

35. Lee YCG. 2022 Synergistic epistasis of the deleterious effects of transposable elements. *Genetics* **220**, iyab211. (doi:10.1093/genetics/iyab211)

36. Matheson J, Masel J. 2024 Background Selection From Unlinked Sites Causes Nonindependent Evolution of Deleterious Mutations. *Genome Biol. Evol.* **16**, evae050. (doi:10.1093/gbe/evae050)

37. Lesecque Y, Keightley PD, Eyre-Walker A. 2012 A Resolution of the Mutation Load Paradox in Humans. *Genetics* **191**, 1321–1330. (doi:10.1534/genetics.112.140343)

38. Eőry L, Halligan DL, Keightley PD. 2010 Distributions of Selectively Constrained Sites and Deleterious Mutation Rates in the Hominid and Murid Genomes. *Mol. Biol. Evol.* **27**, 177–192. (doi:10.1093/molbev/msp219)

39. Wang Y, Obbard DJ. 2023 Experimental estimates of germline mutation rate in eukaryotes: a phylogenetic meta-analysis. *Evol. Lett.* **7**, 216–226. (doi:10.1093/evlett/qrad027)

40. Reed DH. 2005 Relationship between population size and fitness. *Conserv. Biol.* **19**, 235.

41. Kondrashov AS. 2017 *Crumbling Genome: The Impact of Deleterious Mutations on Humans*. New Jersey, US: John Wiley & Sons.

42. Haller BC, Messer PW. 2019 SLiM 3: Forward Genetic Simulations Beyond the Wright–Fisher Model. *Mol. Biol. Evol.* **36**, 632–637. (doi:10.1093/molbev/msy228)

43. McCandlish DM, Epstein CL, Plotkin JB. 2015 Formal properties of the probability of fixation: Identities, inequalities and approximations. *Theor. Popul. Biol.* **99**, 98–113. (doi:10.1016/j.tpb.2014.11.004)

44. Ewens WJ. 2004 Discrete Stochastic Models. In *Mathematical Population Genetics 1: Theoretical Introduction*, pp. 104–109. Springer Science & Business Media.

45. Kim BY, Huber CD, Lohmueller KE. 2017 Inference of the Distribution of Selection Coefficients for New Nonsynonymous Mutations Using Large Samples. *Genetics* **206**, 345–361. (doi:10.1534/genetics.116.197145)

46. Kryukov GV, Schmidt S, Sunyaev S. 2005 Small fitness effect of mutations in highly conserved non-coding regions. *Genetics* **14**, 2221–2229.

47. Di C, Ramesh S, Ernst J, Lohmueller KE. 2025 The landscape of fitness effects of putatively functional noncoding mutations in humans. , 2025.05.14.654124. (doi:10.1101/2025.05.14.654124)

48. VanValen L. 1973 A New Evolutionary Law. *Evol. Theory* **1**, 1–30.

49. Bertram J, Masel J. 2019 Density-dependent selection and the limits of relative fitness. *Theor. Popul. Biol.* **129**, 81–92. (doi:10.1016/j.tpb.2018.11.006)

50. Draghi JA, McGlothlin JW, Kindsvater HK. 2024 Demographic feedbacks during evolutionary rescue can slow or speed adaptive evolution. *Proc. R. Soc. B Biol. Sci.* **291**, 20231553. (doi:10.1098/rspb.2023.1553)

51. Pardo-Manuel de Villena F, Sapienza C. 2001 Recombination is proportional to the number of chromosome arms in mammals. *Mamm. Genome* **12**, 318–322. (doi:10.1007/s003350020005)

52. Kelleher J, Thornton KR, Ashander J, Ralph PL. 2018 Efficient pedigree recording for fast population genetics simulation. *PLOS Comput. Biol.* **14**, e1006581. (doi:10.1371/journal.pcbi.1006581)

53. Higgins K, Lynch M. 2001 Metapopulation extinction caused by mutation accumulation. *Proc. Natl. Acad. Sci.* **98**, 2928–2933. (doi:10.1073/pnas.031358898)

54. Nahum JR, Godfrey-Smith P, Harding BN, Marcus JH, Carlson-Stevermer J, Kerr B. 2015 A tortoise–hare pattern seen in adapting structured and unstructured populations suggests a rugged fitness landscape in bacteria. *Proc. Natl. Acad. Sci.* **112**, 7530–7535. (doi:10.1073/pnas.1410631112)

55. Ronce O, Kirkpatrick M. 2001 When Sources Become Sinks: Migrational Meltdown in Heterogeneous Habitats. *Evolution* **55**, 1520–1531.

56. Olusanya O, Khudiakova K, Sachdeva H. 2025 Genetic Load, Eco-Evolutionary Feedback, and Extinction in Metapopulations. *Am. Nat.* **205**. (doi:10.1086/735562)

57. Gomulkiewicz R, Holt RD. 1995 When does Evolution by Natural Selection Prevent Extinction? *Evolution* **49**, 201–207. (doi:10.2307/2410305)

58. Gonzalez A, Ronce O, Ferriere R, Hochberg ME. 2013 Evolutionary rescue: an emerging focus at the intersection between ecology and evolution. *Philos. Trans. R. Soc. B Biol. Sci.* **368**, 20120404. (doi:10.1098/rstb.2012.0404)

59. Alexander HK, Martin G, Martin OY, Bonhoeffer S. 2014 Evolutionary rescue: linking theory for conservation and medicine. *Evol. Appl.* **7**, 1161–1179. (doi:10.1111/eva.12221)

60. Carlson SM, Cunningham CJ, Westley PAH. 2014 Evolutionary rescue in a changing world. *Trends Ecol. Evol.* **29**, 521–530. (doi:10.1016/j.tree.2014.06.005)

527 61. Bell G. 2017 Evolutionary Rescue. *Annu. Rev. Ecol. Evol. Syst.* **48**, 605–627. (doi:10.1146/annurev-
528 ecolsys-110316-023011)

529 62. Orr HA, Unckless RL. 2008 Population Extinction and the Genetics of Adaptation. *Am. Nat.* **172**,
530 160–169. (doi:10.1086/589460)

531 63. Martin G, Aguilée R, Ramsayer J, Kaltz O, Ronce O. 2013 The probability of evolutionary rescue:
532 towards a quantitative comparison between theory and evolution experiments. *Philos. Trans. R. Soc.*
533 *B Biol. Sci.* **368**, 20120088. (doi:10.1098/rstb.2012.0088)

534 64. Orr HA, Unckless RL. 2014 The Population Genetics of Evolutionary Rescue. *PLoS Genet.* **10**,
535 e1004551. (doi:10.1371/journal.pgen.1004551)

536 65. Uecker H, Otto SP, Hermisson J. 2014 Evolutionary Rescue in Structured Populations. *Am. Nat.* **183**,
537 E17–E35. (doi:10.1086/673914)

538 66. Uecker H, Hermisson J. 2016 The Role of Recombination in Evolutionary Rescue. *Genetics* **202**,
539 721–732. (doi:10.1534/genetics.115.180299)

540 67. Wilson BA, Pennings PS, Petrov DA. 2017 Soft Selective Sweeps in Evolutionary Rescue. *Genetics*
541 **205**, 1573–1586. (doi:10.1534/genetics.116.191478)

542 68. Shaffer ML. 1981 Minimum Population Sizes for Species Conservation. *BioScience* **31**, 131–134.
543 (doi:10.2307/1308256)

544 69. Lacava J, Hughes J. 1984 Determining Minimum Viable Population Levels. *Wildl. Soc. Bull. 1973-*
545 *2006* **12**, 370–376.

546 70. Reed DH, O'Grady JJ, Brook BW, Ballou JD, Frankham R. 2003 Estimates of minimum viable
547 population sizes for vertebrates and factors influencing those estimates. *Biol. Conserv.* **113**, 23–34.
548 (doi:10.1016/S0006-3207(02)00346-4)

549 71. Traill LW, Bradshaw CJA, Brook BW. 2007 Minimum viable population size: A meta-analysis of 30
550 years of published estimates. *Biol. Conserv.* **139**, 159–166. (doi:10.1016/j.biocon.2007.06.011)

551 72. Nabutanyi P, Wittmann MJ. 2022 Modeling minimum viable population size with multiple genetic
552 problems of small populations. *Conserv. Biol.* **36**, e13940. (doi:10.1111/cobi.13940)

553 73. Nunney L, Campbell KA. 1993 Assessing minimum viable population size: Demography meets
554 population genetics. *Trends Ecol. Evol.* **8**, 234–239. (doi:10.1016/0169-5347(93)90197-W)

555 74. IUCN. 2025 The IUCN Red List of Threatened Species. *IUCN Red List Threat. Species*. See
556 https://www.iucnredlist.org (accessed on 3 October 2025).

557 75. Pacifici M *et al.* 2015 Assessing species vulnerability to climate change. *Nat. Clim. Change* **5**, 215–
558 224. (doi:10.1038/nclimate2448)

559 76. Santidrián Tomillo P, Wallace BP, Paladino FV, Spotila JR, Genovart M. 2021 Short-term gain, long-
560 term loss: How a widely-used conservation tool could further threaten sea turtles. *Biol. Conserv.* **261**,
561 109260. (doi:10.1016/j.biocon.2021.109260)

562 77. Rout TM, Hauser CE, Possingham HP. 2007 Minimise long-term loss or maximise short-term gain?:
563 Optimal translocation strategies for threatened species. *Ecol. Model.* **201**, 67–74.
564 (doi:10.1016/j.ecolmodel.2006.07.022)

565 78. Bottrill MC *et al.* 2008 Is conservation triage just smart decision making? *Trends Ecol. Evol.* **23**, 649–
566 654. (doi:10.1016/j.tree.2008.07.007)

567 79. Vucetich JA, Nelson MP, Bruskotter JT. 2017 Conservation Triage Falls Short Because Conservation
568 Is Not Like Emergency Medicine. *Front. Ecol. Evol.* **5**. (doi:10.3389/fevo.2017.00045)

569 80. Willis KJ, Birks HJB. 2006 What Is Natural? The Need for a Long-Term Perspective in Biodiversity
570 Conservation. *Science* **314**, 1261–1265. (doi:10.1126/science.1122667)

571 81. Barnosky AD *et al.* 2017 Merging paleobiology with conservation biology to guide the future of
572 terrestrial ecosystems. *Science* **355**, eaah4787. (doi:10.1126/science.aah4787)

573 82. Whiteley AR, Fitzpatrick SW, Funk WC, Tallmon DA. 2015 Genetic rescue to the rescue. *Trends*
574 *Ecol. Evol.* **30**, 42–49. (doi:10.1016/j.tree.2014.10.009)

575 83. Frankham R, Ballou JD, Ralls K, Eldridge M, Dudash MR, Fenster CB, Lacy RC, Sunnucks P. 2017
576 *Genetic Management of Fragmented Animal and Plant Populations*. Oxford U.K.: Oxford University
577 Press.

578 84. Bell DA, Robinson ZL, Funk WC, Fitzpatrick SW, Allendorf FW, Tallmon DA, Whiteley AR. 2019
579 The Exciting Potential and Remaining Uncertainties of Genetic Rescue. *Trends Ecol. Evol.* **34**, 1070–
580 1079. (doi:10.1016/j.tree.2019.06.006)

581 85. Ralls K, Ballou JD, Dudash MR, Eldridge MDB, Fenster CB, Lacy RC, Sunnucks P, Frankham R.
582 2018 Call for a Paradigm Shift in the Genetic Management of Fragmented Populations. *Conserv. Lett.*
583 **11**, e12412. (doi:10.1111/conl.12412)

584 86. Ralls K, Sunnucks P, Lacy RC, Frankham R. 2020 Genetic rescue: A critique of the evidence supports
585 maximizing genetic diversity rather than minimizing the introduction of putatively harmful genetic
586 variation. *Biol. Conserv.* **251**, 108784. (doi:10.1016/j.biocon.2020.108784)

587 87. Bijlsma R, Westerhof MDD, Roekx LP, Pen I. 2010 Dynamics of genetic rescue in inbred Drosophila
588 melanogaster populations. *Conserv. Genet.* **11**, 449–462. (doi:10.1007/s10592-010-0058-z)

589 88. Pérez-Pereira N, Caballero A, García-Dorado A. 2022 Reviewing the consequences of genetic
590 purging on the success of rescue programs. *Conserv. Genet.* **23**, 1–17. (doi:10.1007/s10592-021-
591 01405-7)

592 89. Chen N, Cosgrove EJ, Bowman R, Fitzpatrick JW, Clark AG. 2016 Genomic Consequences of
593 Population Decline in the Endangered Florida Scrub-Jay. *Curr. Biol.* **26**, 2974–2979.
594 (doi:10.1016/j.cub.2016.08.062)

595 90. 2025 MaselLab/MutationLoad: C1.0.0. (doi:10.5281/zenodo.17281300)

596